Doc. - SRI file

~~[illegible]~~

CR 73156

STANFORD RESEARCH INSTITUTE

MENLO PARK, CALIFORNIA

August 23, 1965

Report No. 13, SRI Project No. PHU-5093

Interim Report

CRYOGENIC MAGNETOMETER DEVELOPMENT

Prepared for

National Aeronautics and Space Administration
Ames Research Center
Moffett Field, California

Attn: Contracting Officer

Contract NAS2-2088

GPO PRICE $ ________

CFSTI PRICE(S) $ ________

Hard copy (HC) 3.00

Microfiche (MF) ________

ff 653 July 65

This is an Interim Report presented to cover the long-term stability test and temperature sensitivity test of two of the Ames Sensors. These tests, to be discussed and interpreted in this report, show that the Ames flux gate sensor is very stable over long time periods, e.g., drifting less than 1 μgauss in a 10-hour period, and that observed sensor drift is always associated with a sensor temperature change. Further, the tests show that the temperature coefficient of the sensor is probably not a simple linear function of temperature during temperature changes, but that the average steady state coefficient is about -0.4 μgauss/$^{\circ}$C.

The long-term stability test was conducted from May 25 to 31, 1965. During this test a continuous record was made of the output from the two sensors and of the following significant external variables:

1. Environmental air temperature of the sensors

2. Room temperature

3. Vertical component of the external magnetic field at the superconducting magnetic shield

4. Superconducting shield temperature

5. Output voltage from both sensor power supplies

The test environment was provided by the superconducting magnetic shield which has been thoroughly described in previous monthly and midterm reports. Figure 1 is an axial magnetic field map of this test environment immediately before the start of the long-term stability test. Figure 2 is a schematic diagram of the test facility showing the placement of all measuring instruments.

Sensor Temperature Environment

The control and measurement of the temperature environment of the Ames sensors is of particular importance. Figure 3 shows the two different control systems used during the test. For the system shown in Part a, Fig. 3, the sensor temperature was initially controlled by blowing room temperature air down past the Linde dewar wall and up through the 1-in. diameter acrylic tube that positioned the sensors. Temperature measurement was with a thermistor placed at the outlet end of the 1-in. acrylic tube. In this case it is apparent that the room temperature air would be cooled by contact with the dewar wall, thus the sensors should be a few degrees cooler than room temperature. Part way through the test this system was modified to pull air from the room through the 1-in. acrylic tube, past the sensors, and then past the Linde dewar wall and back to the room. Deliberate sensor temperature changes were caused by heating or cooling the air used to regulate the sensor temperature. This method of temperature measurement is, of course, indirect, but was used since it avoided placing magnetic material or current-carrying wires near the Ames sensors.

During the initial phase of the test it became apparent that the sensor reading was temperature sensitive, and in an attempt to separate dewar wall temperature control from sensor temperature control, we constructed the system shown in Part b, Fig. 3. By this temperature control separation we could determine if thermal emf's in the aluminum dewar wall were causing the observed temperature effects. As shown in Fig. 3, the dewar wall temperature was measured with a second thermistor which had been used to measure room temperature. Also evident from the airflow in this new system is that the sensor air temperature should be very close to room temperature.

The Ames sensors had to be removed from the superconducting shield during the installation of the new temperature control apparatus. Upon reinstalling the sensors and accurately placing them at the original axial position in the shield, we observed no significant shift in the average sensor reading. This indicates that the acrylic tubes used for the temperature control systems are very nearly nonmagnetic, since we had changed from 1 to 3 concentric acrylic tubes without measurably affecting the magnetic field.

Explanation of Instruments - Ames Sensor

Each sensor was connected to its individual electronic package and its separate power supply. The power supplies were fed from a recently charged, large, 12-vdc storage battery. The voltage from the power supplies

Fig. 1. MAGNETIC FIELD MAP ALONG THE AXIS OF THE SUPERCONDUCTING SHIELD. This shows the general field configuration during the stability test. It was made with the No. 1 sensor mounted with its tip down. The locations of the sensors during the stability test are also shown.

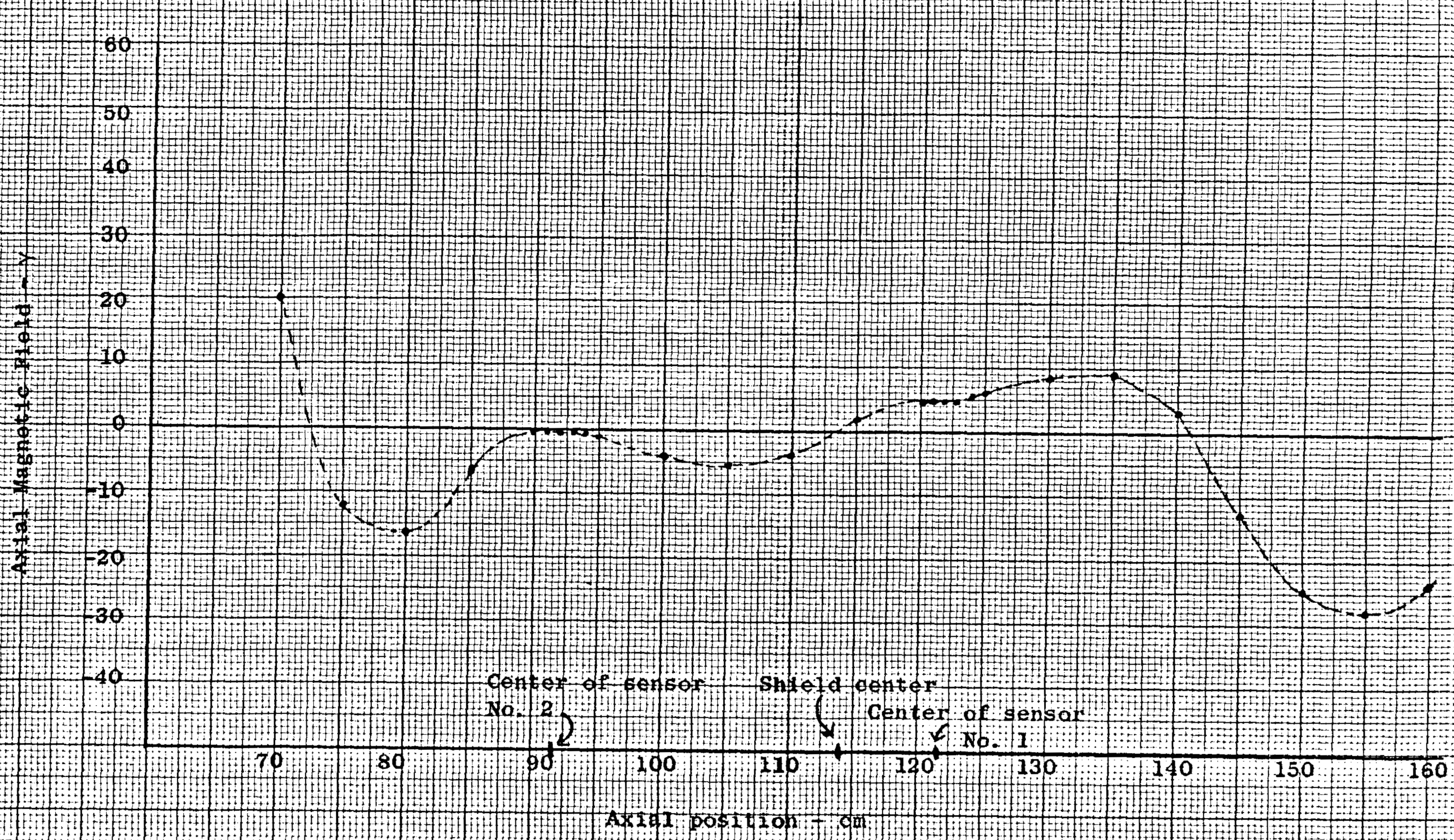

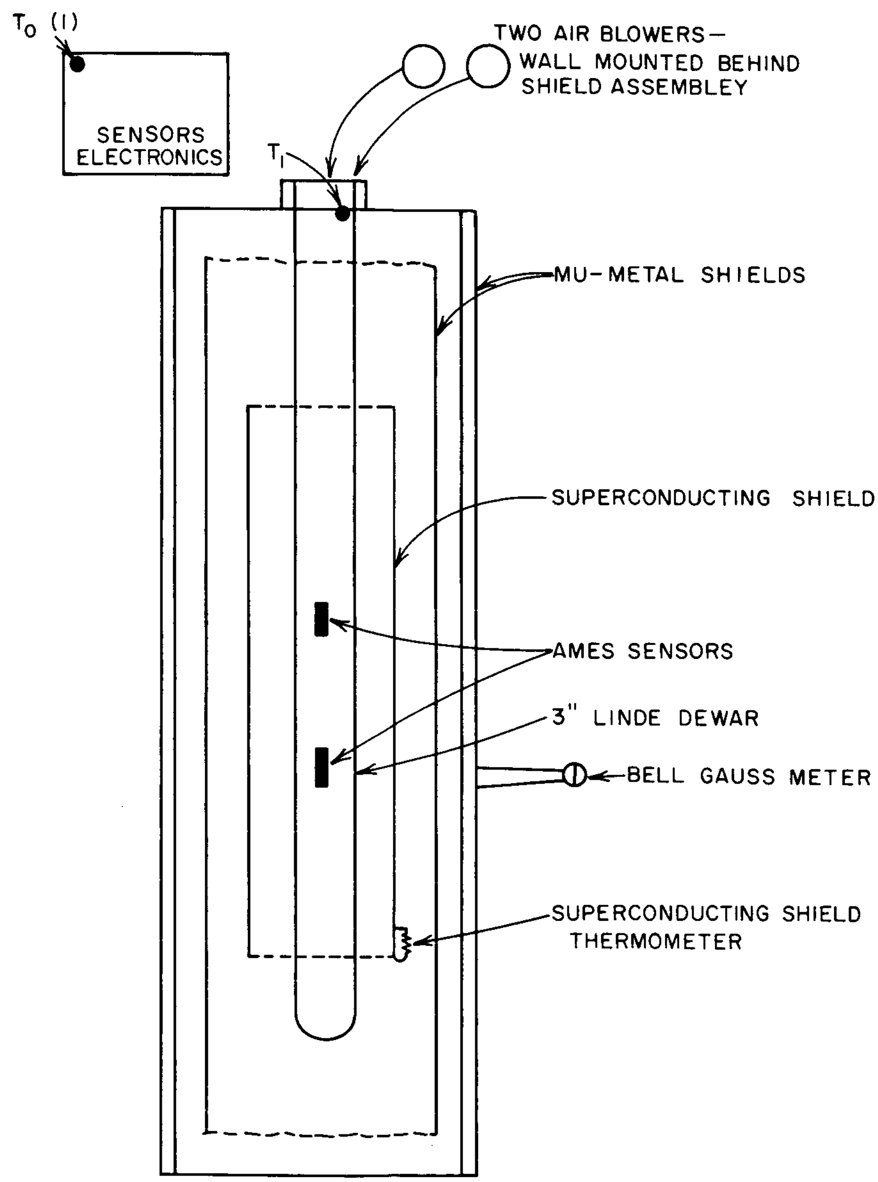

FIG. 2 TEST FACILITY FOR LONG TERM STABILITY TEST

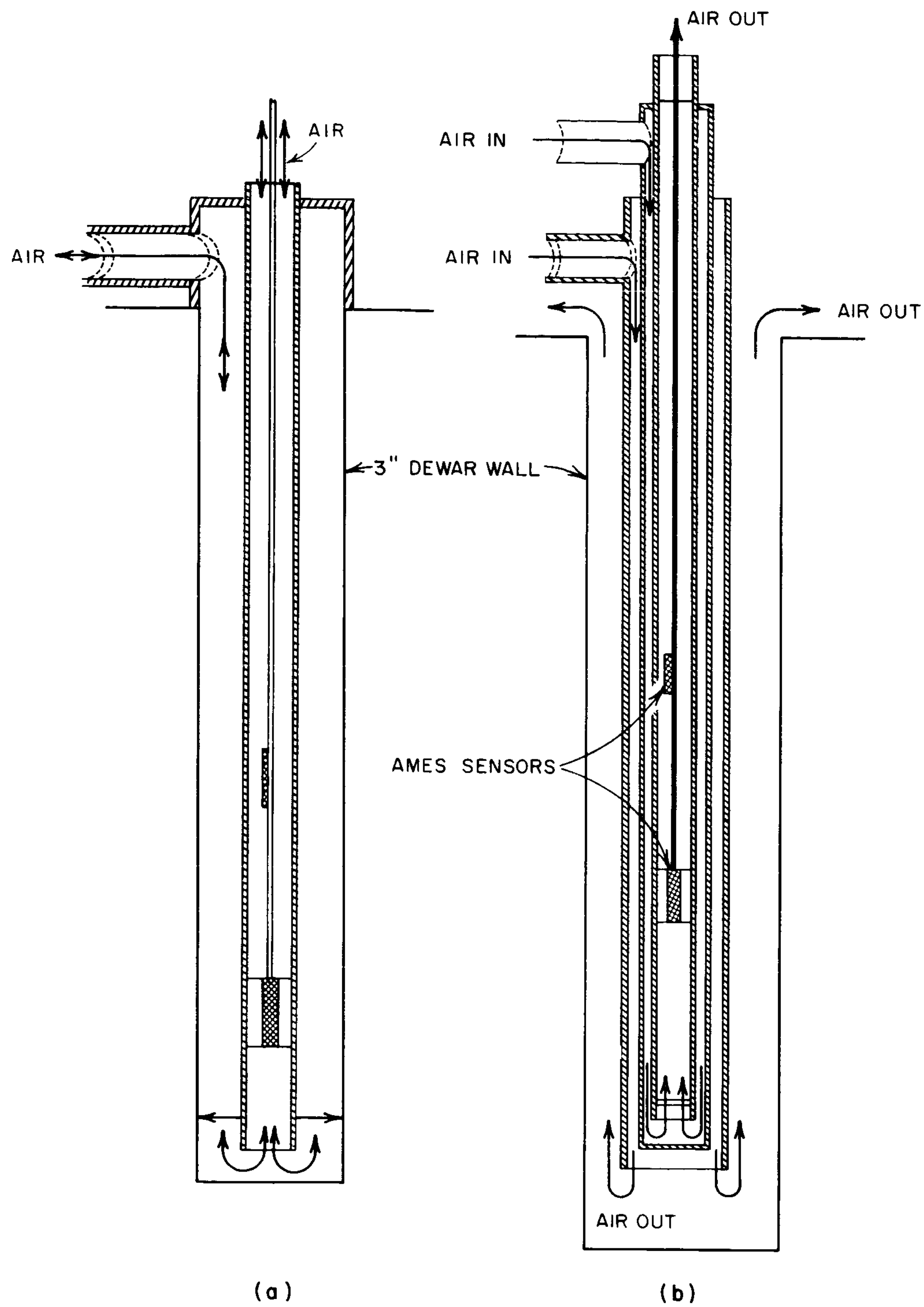

FIG. 3 SENSOR TEMPERATURE CONTROL SYSTEMS

to the sensor electronics was read through a d-c bridge connection. The supply voltage should be 7.20 vdc. The accuracy of our data was ±12 mvdc, thus these data show voltage variations within ±½% of the standard reading.

Each sensor output was continuously read with a Bausch and Lomb pen recorder which has a 1-cps response time. Each recorder was fitted with an automatic timer that disconnected the sensor and shorted the recorder input terminals for a zero calibration and then put in a standard 28.6-mvdc gain calibration signal (2.86 gamma) every hour. These recorder charts were then manually read every 1 to 2 hours to accurately reproduce any fluctuations, and punched on IBM data cards. The reading accuracy was ±¼ μgauss.

Explanation of Instruments - Other Instruments

The superconducting shield temperature was measured with a 1/10-w, 100-ohm, nominal Allen-Bradley carbon resistor read with an a-c bridge.

The thermistors were Globar Model A 1406P-1, 650-ohm ±20% at 37.8°C, with a +10%/°C temperature coefficient. A constant voltage power supply maintained 4.2 vdc across each thermistor, and the current was measured directly with the galvnometer on the Visicorder. The external magnetic field was measured with a Bell Model 240 differential gaussmeter. This is a Hall-effect device which has a feedback circuit to balance the ambient field, allowing deviations to be read about this balance point. We used the 100-mgauss full-scale range in monitoring the external field fluctuations.

All of these variables were continuously recorded on a 10-channel Visicorder. The Visicorder record was read with an Oscar chart reader at 1- or 5-minute intervals, again depending on the interval required to accurately reproduce the data. Reading accuracy was approximately ±1/20 in. The sensitivity of each channel and its resultant accuracy is given in the following table:

Channel Function	Sensitivity	Accuracy of Data
Superconducting shield temperature	43 milli°C/in.	±2 milli°C
Thermistor - dewar wall temperature	1.48°C/in.	±74 milli°C
Thermistor - sensor temp.	1.16°C/in.	±58 milli°C
Bell magnetometer	335.0 mgauss/in.	±1.75 mgauss
No.1 sensor supply voltage	0.236 vdc/in.	±11.8 mvdc
No.2 sensor supply voltage	0.236 vdc/in.	±11.8 mvdc

Analysis of the Long-Term Stability Test Data

The results of this test must be interpreted with knowledge of the properties of the superconducting magnetic shield, temperature, and magnetic field effects on the various measuring instruments and environmental conditions during the experiment.

The detailed chronology shown in Table I describes the significant environmental changes which occurred during the stability test. The major changes were during liquid helium transfers when the air temperature near the shield was cooled by the helium boil-off gas and the ambient external magnetic field was changed by the presence of the large helium storage dewar, and intentional sensor temperature changes.

An initial examination of the experimental data showed that the superconducting shield temperature did not vary more than $\pm 0.040^{\circ}C$. Intentional temperature changes of the shield by as much as $0.5^{\circ}C$ had no observable effect on the Ames sensor readings so we can safely conclude that the temperature fluctuations of the superconducting shield during the stability test had no measurable effect on the magnetic field. Thus the shield temperature was not read from the Visicorder record and is not available on data cards. The Visicorder record is available though, showing the complete shield temperature plot.

The two sensor supply voltage readings were plotted and showed a linear decrease in voltage with time which amounted to about 0.1 vdc over the full test. These data are not shown here due to the simple linear time dependence.

The experimental results, as recorded on data cards, are shown in Fig. 4. Here we show both sensor readings and the sensor temperature. The chronology of events which occurred during the experiment are shown in Table I. The time axis of this plot is greatly compressed and makes it difficult to interpret the data. Thus these same data have been plotted again with an expanded time axis as shown on Figs. 5 through 9. These figures include the recorder zero and gain calibration signals for both sensors. Also the air temperature has been plotted with a smaller temperature scale than on Fig. 4. Room temperature was approximately equal to the sensor air temperature except during the noted intervals where the sensor temperature was intentionally varied.

An attempt to obtain an average temperature coefficient for each sensor and to correlate the variations of the sensor readings with temperature and external magnetic field was made as follows.

Table I

CHRONOLOGY OF LONG-TERM STABILITY TEST

Time	
2555 (1605 Tues., May 25,1965)	Start of fully instrumented stability test
2560	Prepare for helium transfer
2565	Start helium transfer
2605	End helium transfer
2662	Sensor No. 2 chart recorder inoperative
3555	Liquid N_2 dewar brought near shield
3610	Sensor No. 2 back on
3620	Heat superconducting shield with resistor $-1/2^{o}C$
3665	Warm air onto sensors
3675	Warm air off
3690	Sensor temperature change - turn off sensor blower
3700	End temperature change
3830	Turn off sensor air blower
3842	Turn back on to pull air through sensor tube
3880	Start helium transfer
3928	Stop helium transfer
4000	Sensor No. 2 inoperative
4090	Changed suction hose for sensor air supply
4114	Sensor No. 2 on
4352	Sensor No. 2 chart recorder inoperative
4984	Sensor No. 2 back on
5310	Helium transfer started
5400	Stop helium transfer
5500	Warm air on electronics
5520	Transfer helium again
6680	Start helium transfer
6725	End helium transfer
7280	Stopped Visicorder during change of temperature control system. Sensor No. 2 inoperative
7325	Begin new sensor temperature control. Bell gaussmeter inoperative
7345	Begin helium transfer
7350	Transfer line plugged
7372	End helium transfer
7928	Sensor No. 2 back on
7932	Turn off dewar blower
7934	Turn on dewar blower
7935	Turn off sensor blower
7938	Turn on sensor blower
7990	Start Bell gaussmeter
8306 8346	Numbers 1 and 2 sensors off
8351	Dewar blower off
8354	Hot air blower into dewar blower
8387	End helium transfer
8610	Temperature change on sensors
8630	End temperature change on sensors
8635	Start helium transfer
8665	Stop helium transfer
10090	Helium transfer
10890	Temperature change on sensors

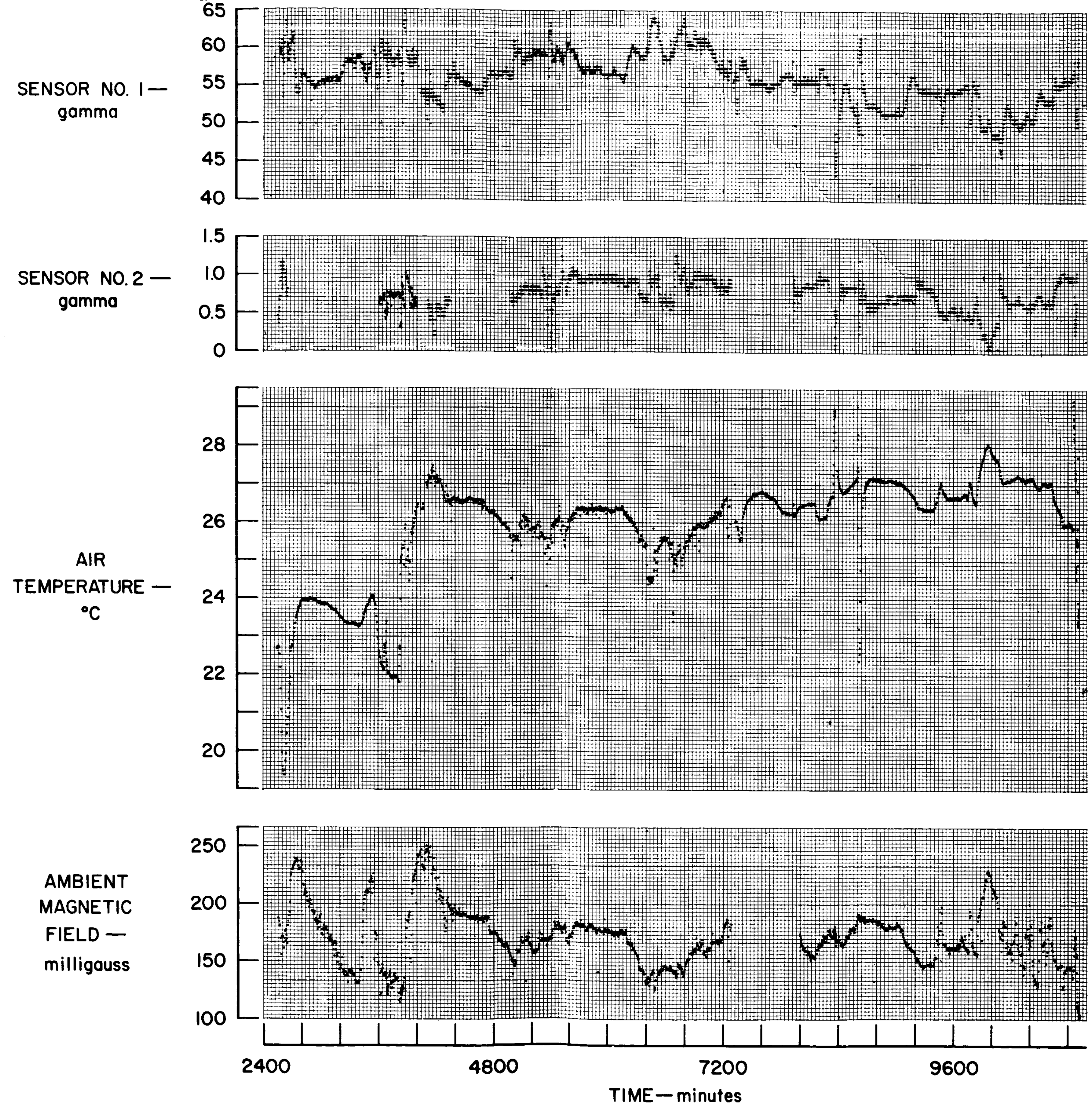
SENSOR NO. 1 — gamma
65
60
55
50
45
40
SENSOR NO. 2 — gamma
1.5
1.0
0.5
0
AIR TEMPERATURE — °C
28
26
24
22
20
AMBIENT MAGNETIC FIELD — milligauss
250
200
150
100
2400
4800
7200
9600
TIME — minutes

FIG. 4

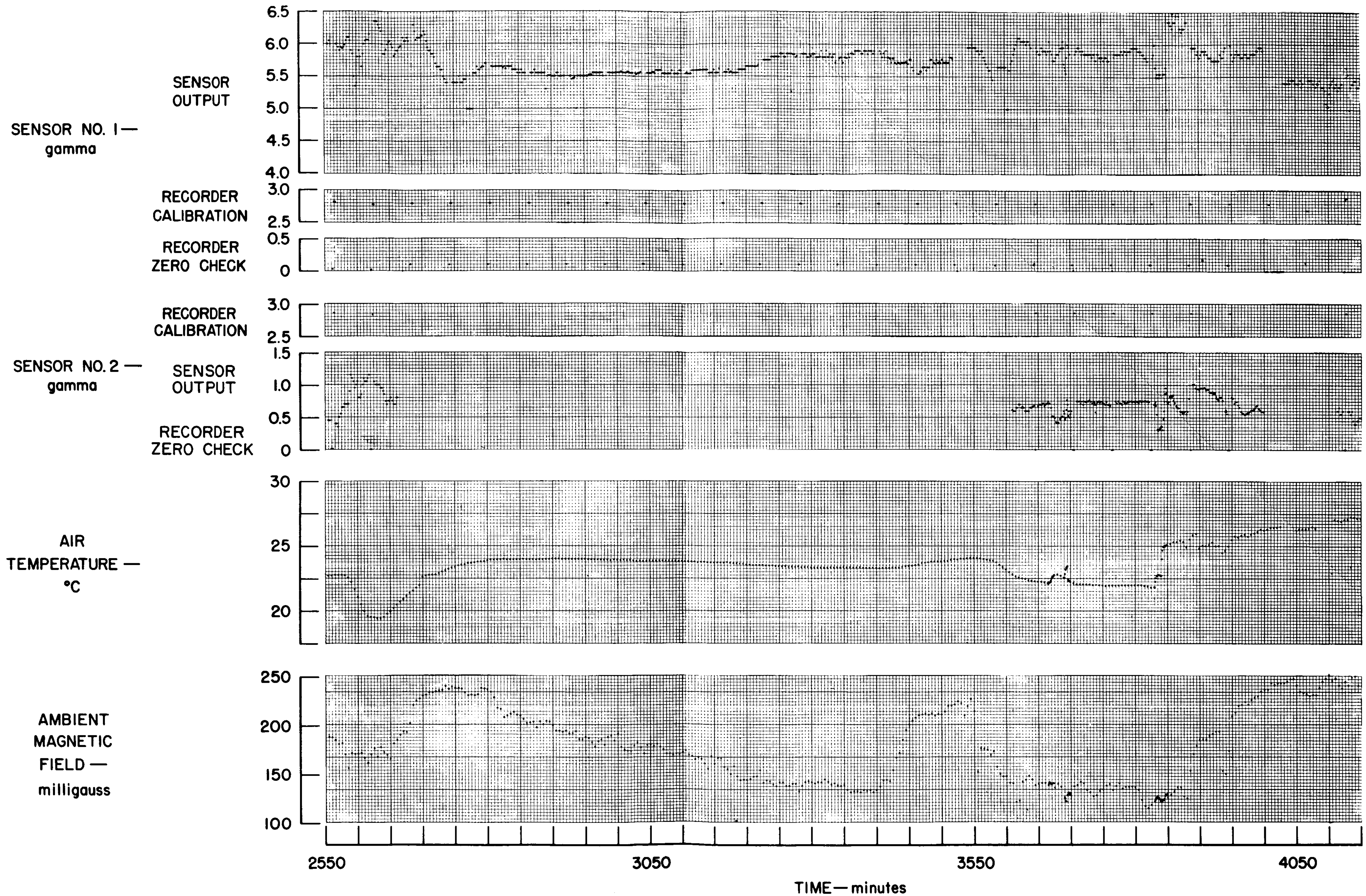
SENSOR NO. 1 — gamma
SENSOR OUTPUT
6.5
6.0
5.5
5.0
4.5
4.0
RECORDER CALIBRATION
3.0
2.5
RECORDER ZERO CHECK
0.5
0
SENSOR NO. 2 — gamma
RECORDER CALIBRATION
3.0
2.5
SENSOR OUTPUT
1.5
1.0
0.5
RECORDER ZERO CHECK
0
AIR TEMPERATURE — °C
30
25
20
AMBIENT MAGNETIC FIELD — milligauss
250
200
150
100
2550
3050
3550
4050
TIME — minutes

FIG. 5

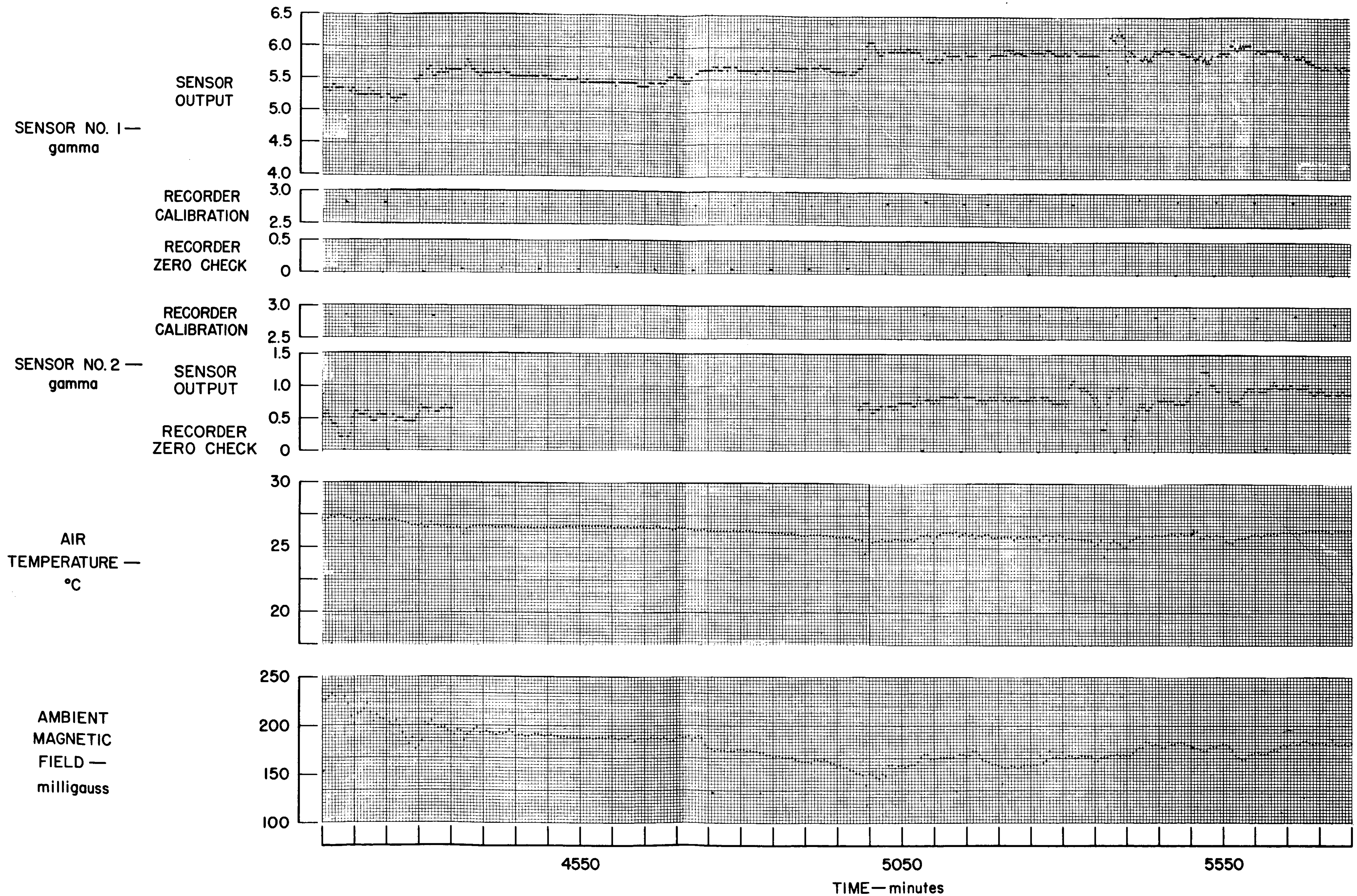
SENSOR NO. 1 — gamma
SENSOR OUTPUT
RECORDER CALIBRATION
RECORDER ZERO CHECK
SENSOR NO. 2 — gamma
RECORDER CALIBRATION
SENSOR OUTPUT
RECORDER ZERO CHECK
AIR TEMPERATURE — °C
AMBIENT MAGNETIC FIELD — milligauss
6.5
6.0
5.5
5.0
4.5
4.0
3.0
2.5
0.5
0
3.0
2.5
1.5
1.0
0.5
0
30
25
20
250
200
150
100
4550
5050
5550
TIME — minutes

FIG. 6

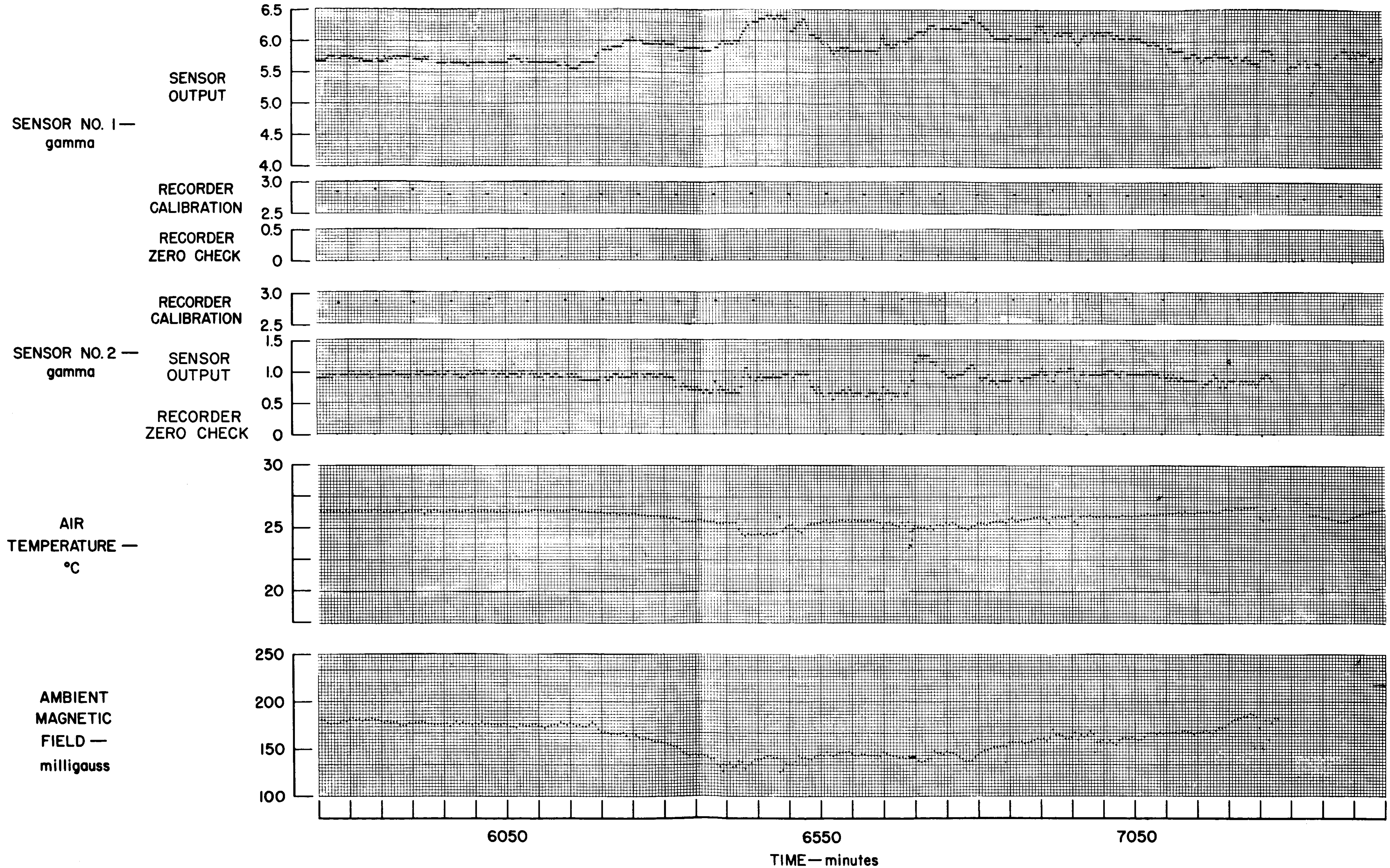
SENSOR NO. 1 — gamma
SENSOR OUTPUT
RECORDER CALIBRATION
RECORDER ZERO CHECK
SENSOR NO. 2 — gamma
RECORDER CALIBRATION
SENSOR OUTPUT
RECORDER ZERO CHECK
AIR TEMPERATURE — °C
AMBIENT MAGNETIC FIELD — milligauss
6.5
6.0
5.5
5.0
4.5
4.0
3.0
2.5
0.5
0
3.0
2.5
1.5
1.0
0.5
0
30
25
20
250
200
150
100
6050
6550
7050
TIME — minutes

FIG. 7

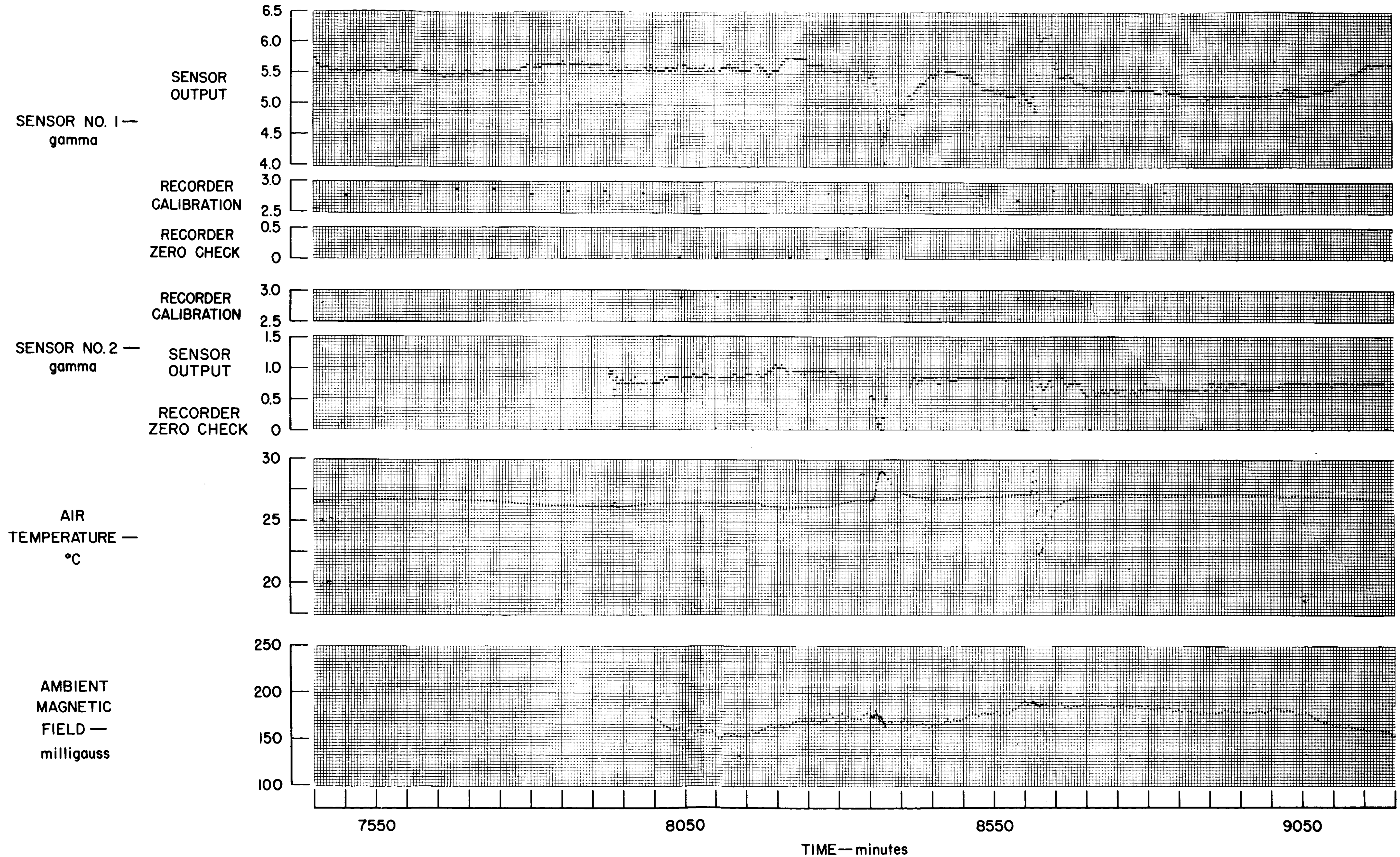
SENSOR NO. 1 — gamma
SENSOR OUTPUT
RECORDER CALIBRATION
RECORDER ZERO CHECK
SENSOR NO. 2 — gamma
RECORDER CALIBRATION
SENSOR OUTPUT
RECORDER ZERO CHECK
AIR TEMPERATURE — °C
AMBIENT MAGNETIC FIELD — milligauss
6.5
6.0
5.5
5.0
4.5
4.0
3.0
2.5
0.5
0
3.0
2.5
1.5
1.0
0.5
0
30
25
20
250
200
150
100
7550
8050
8550
9050
TIME — minutes

FIG. 8

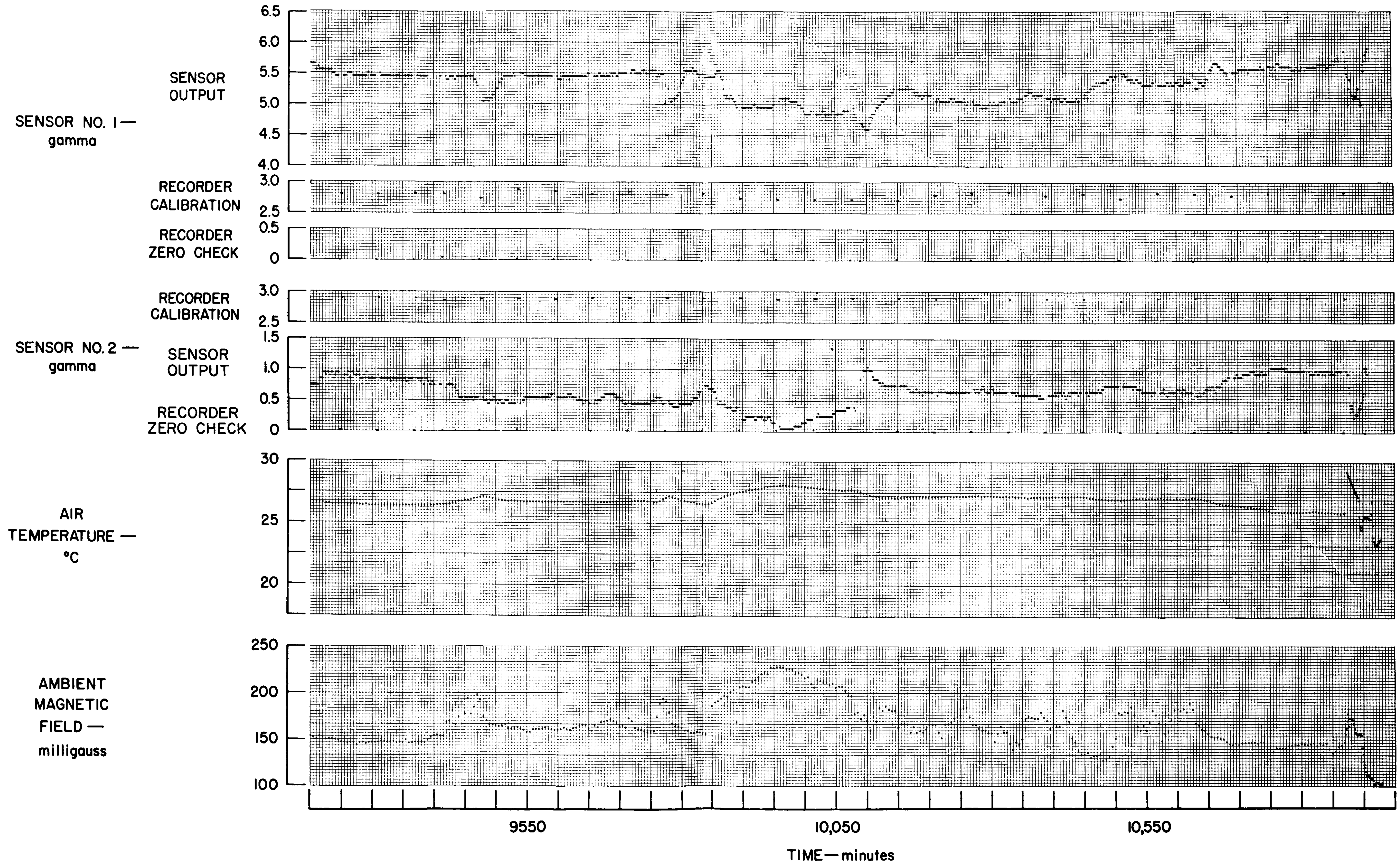
SENSOR NO. 1 —
gamma
SENSOR
OUTPUT
6.5
6.0
5.5
5.0
4.5
4.0
RECORDER
CALIBRATION
3.0
2.5
RECORDER
ZERO CHECK
0.5
0
RECORDER
CALIBRATION
3.0
2.5
SENSOR NO. 2 —
gamma
SENSOR
OUTPUT
1.5
1.0
0.5
RECORDER
ZERO CHECK
0
AIR
TEMPERATURE —
°C
30
25
20
AMBIENT
MAGNETIC
FIELD —
milligauss
250
200
150
100
9550
10,050
10,550
TIME — minutes

FIG. 9

The No. 1 Ames sensor record was used as a standard for the time interval between readings. The other channels, i.e., sensor No. 2, sensor temperature, and external magnetic field, were interpolated by a computer to give synchronous readings with sensor No. 1.

An approximate temperature coefficient was obtained for each Ames sensor as follows: A region of constant magnetic field reading and constant temperature was selected from the preliminary data for each sensor (γ_0 and T_0). The temperature coefficient was then computed as

$$\alpha_i = \frac{\gamma_{io} - \gamma_i(t)}{T_o - T(t)}$$

where $\gamma_i(t)$ = sensor reading at time t
$T(t)$ = sensor temperature at time t
i = sensor No. 1 or 2

We used three different temperature control methods during the test. Thus we computed a different set of α_i's for each region using different γ_{io}'s and T_o's. The α_i's over each time range (temperature control method) were then numerically averaged to give an average to sensor temperature coefficient for that particular time interval.

The sensor readings were then corrected using the average α_i's ($\bar{\alpha}_i$) as follows:

$$\gamma_{i\ \text{corrected}} = \gamma_i(t) + \alpha_i \Delta T$$

where $\gamma_i(t)$ = measured magnetic field at sensor i at time t
$\Delta T = T_o - T(t)$.

The calculations described above were in error for the first part of the stability test data due to a computer programming mistake. The calculations were correct for approximately the last half of the test, and it was clear from the data that a simple point-by-point linear temperature coefficient could not account for the observed variations in the Ames sensor reading. It should be noted, as discussed on Page 1 of this report, that the method of sensor temperature measurement was not direct. Thus it is possible that the incomplete correlation of short term sensor drift with the measured temperature is an instrumental effect. The long term sensor drifts are closely correlated as is evident from Fig. 4.

General Conclusions and Results

The use of the temperature control system shown in Fig. 3-b showed that temperature changes of the dewar wall did not affect the sensor reading. Further support of this conclusion is given in the following section on the sensor temperature sensitivity test.

Conclusions regarding the temperature and external magnetic field correlations can best be made from a close examination of Figs. 5 through 9. All recorded data have been shown on the figures and intervals where no data appear are when the instrument was inoperative as noted on the chronology.

The time interval from 2800 to 3250 on Fig. 5 shows large external magnetic field variations with constant sensor temperature and output. This indicates that the superconducting shield is effective in shielding at least 100 mgauss external field variations. This is in good agreement with our previously reported attenuation coefficients of 10^5 to 10^6 for the superconducting shield alone. From time 3850 to 4150 we changed the sensor temperature control air flow, causing a temperature change of about $+5^{\circ}$C. This caused a permanent sensor output change of approximately 0.4 gamma.

A region where all readings are constant is shown on Fig. 7 from 5750 to 6150. It is clear from this figure that the sensor readings are constant within 0.1 gamma for almost 7 hours where the temperature was held constant.

Intentional sensor temperature variations are shown on Fig. 8 from time 8350 to 8650. The negative sensor temperature coefficient is particularly evident. It is difficult to make precise estimates of the magnitude of the coefficient or the equilibration time of the sensor due to the method used in measuring and controlling the temperature.

The figures also show a definite correlation between the average sensor temperature, which as approximately equal to room temperature except during intentional variations, and the external magnetic field.

We measured the gaussmeter temperature coefficient after the stability test and found a positive coefficient of 16.5 milligauss/$^{\circ}$C at ambient fields of 180 milligauss. This shows that the gaussmeter is as sensitive to temperature variation as the thermistor actually used for the temperature measurement. Precise temperature correction of the external field data is not possible due to the lack of very accurate temperature data at the sensing element.

Test of Temperature Sensitivity of the Ames Sensors

Definite correlations between the temperature of the air used to regulate the sensor temperature and the sensor reading were observed during the long-term stability test. In an effort to accurately investigate the nature of this temperature dependence and separate it from temperature variations of the Linde dewar wall, etc., we built the temperature control system shown in Fig. 10. In this apparatus the two sensors were placed 30-cm apart (as in the long-term stability test), and each sensor was in a separate temperature-controlled water bath. The sensors were protected from direct water contact by thin rubber sleeves as shown in Fig. 10. Water entered the control volume through the lower tubes (A and B) and was syphoned off at the upper tubes (C and D). The axial magnetic field of the superconducting shield immediately before the test is shown in Fig. 11.

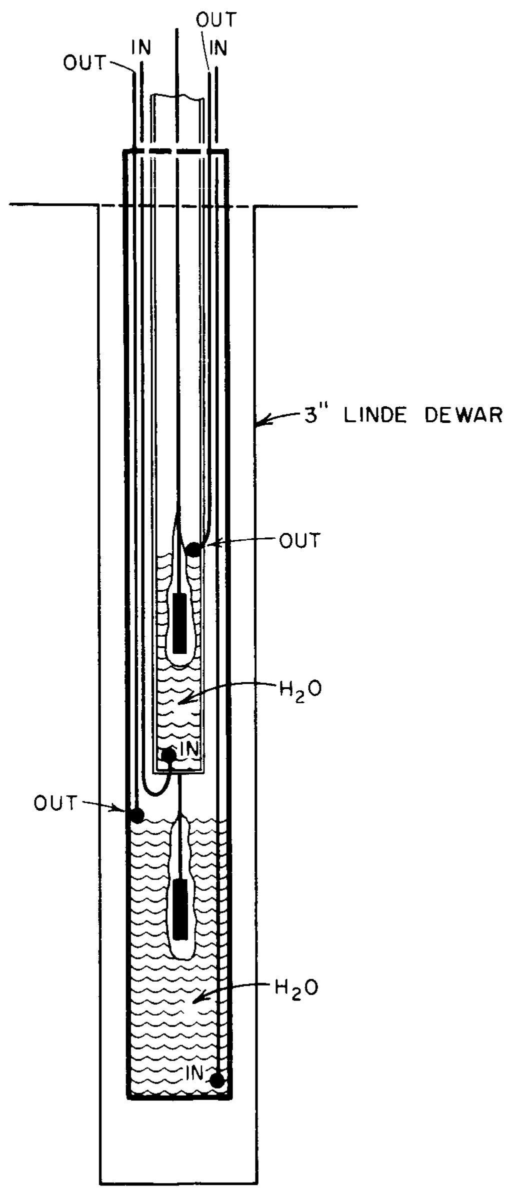

FIG. 10 SENSOR TEMPERATURE CONTROL SYSTEMS

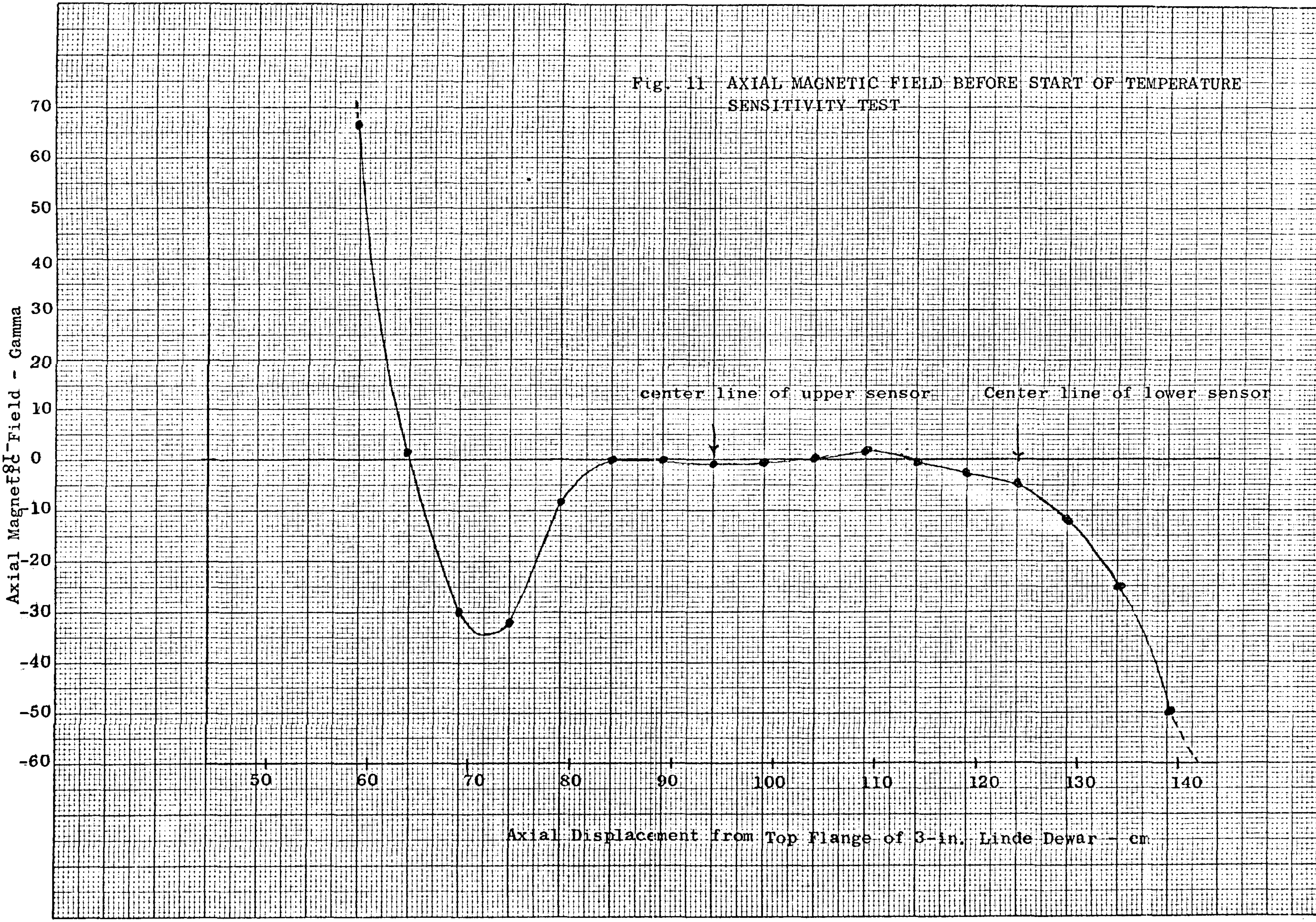

Fig. 11 AXIAL MAGNETIC FIELD BEFORE START OF TEMPERATURE SENSITIVITY TEST

During the test the lower sensor was kept at a constant temperature by circulating cold tap water (22°C). The temperature of the upper sensor was varied from 21°C to 55°C by varying the amount of hot water that was mixed with cold water. We attempted one experiment when the lower sensor was heated but heat rising from the lower bath made temperature control of the upper bath very difficult.

The actual sensor temperature was obtained from measurements of the resistance of the sensor feedback coil. To make this measurement we disconnected the sensors, one at a time, and measured the coil resistance with an a-c bridge. Only a few microwatts of power are required for an accurate temperature measurement. The temperature coefficient of the feed back coil of No. 1 sensor was measured by placing the sensor in thermal baths at known temperatures and measuring the coil resistance as above. These data are shown in Fig. 12. The coefficient is very linear and is equal to 1.99°C/ohm over the range studied (from +20 to +47°C).

The sensor field sensitivity was measured frequently during the experiment by turning on a small field using the d-c transformer and the niobium solenoid of the superconducting magnetic shield assembly.

Results

Figures 13 and 14 show plots of the sensor reading, the sensor temperature, and the magnetic field sensitivity versus time. During the initial 40 to 50 minutes the water temperature and the sensor readings were not stable. The approximate temperature coefficients of sensor No. 2 can be determined from Fig. 14. At time = 165 min we attempted to change the temperature of sensor No. 1, but this was not successful as discussed earlier. Figure 15 is a graph of the average sensor reading versus sensor temperature for sensor No. 2. Figure 16 is the actual recorded trace of the upper Ames sensor for the time interval 95 to 124. This figure shows the equilibrium sensor record at two different temperatures, the region of temperature measurement, sensitivity measurements, and in particular, the increased noise during a temperature change.

The general conclusion reached from these data is that the Ames sensor output is sensitive to temperature. For large ($\simeq$30°C) steady state temperature changes the measured coefficient runs approximately -0.4 μgauss/°C. Further, we have shown that the magnetic field sensitivity is not temperature dependent within the temperature and field range studied, i.e., 30 to 55°C and 0 to 4 gamma.

William S. Goree

William S. Goree
Physicist
Nuclear Physics Department

Approved

T. O. Passell

T. O. Passell for
E. M. Kinderman, Manager
Nuclear Physics Department

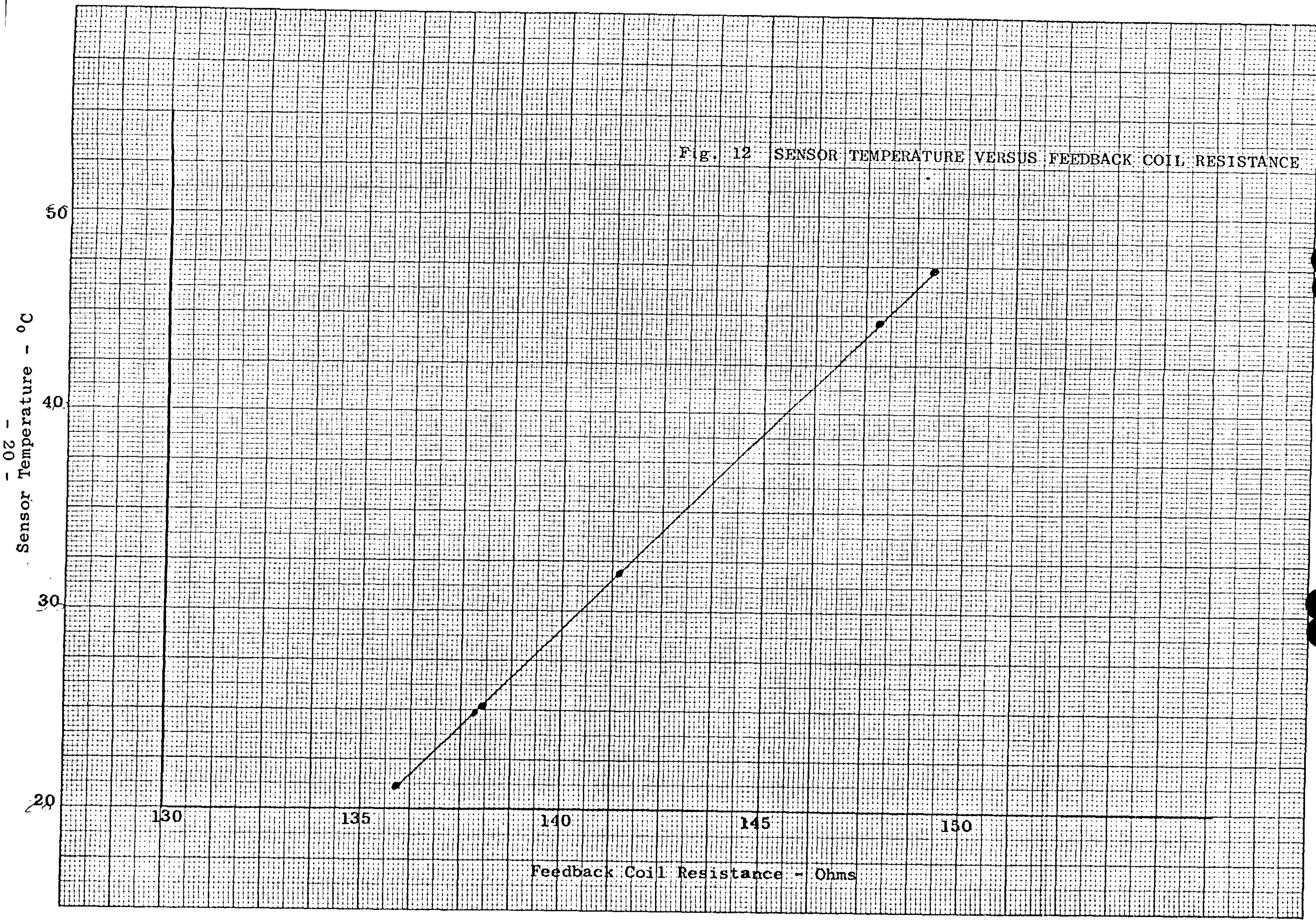

Fig. 12 SENSOR TEMPERATURE VERSUS FEEDBACK COIL RESISTANCE
50
40
30
20
130
135
140
145
150
Feedback Coil Resistance - Ohms
Sensor Temperature - °C

Fig. 13 SENSOR NO. 1 DATA FROM STUDY OF TEMPERATURE DEPENDENCE
Magnetic field sensitivity-γ
4
3
2
Temperature-°C
40
30
20
Sensor output-γ
-2
-1
0
+1
+2
0 10 20 30 40 50 60 70 80 90 100 110 120 130 140 150 160 170 180 190 200 210
Time - minutes

Fig. 14 SENSOR NO. 2 DATA FROM STUDY OF THE TEMPERATURE DEPENDENCE

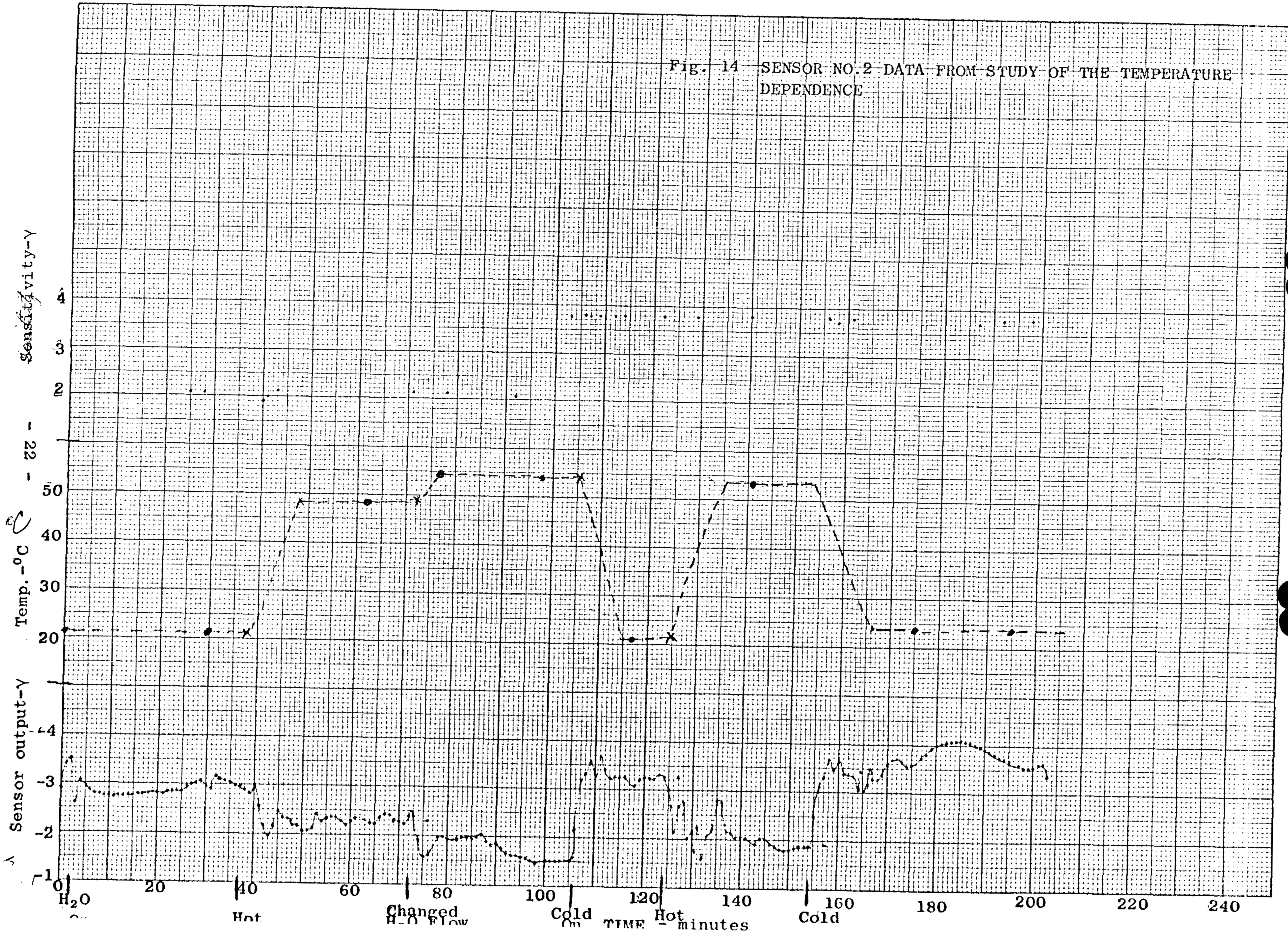

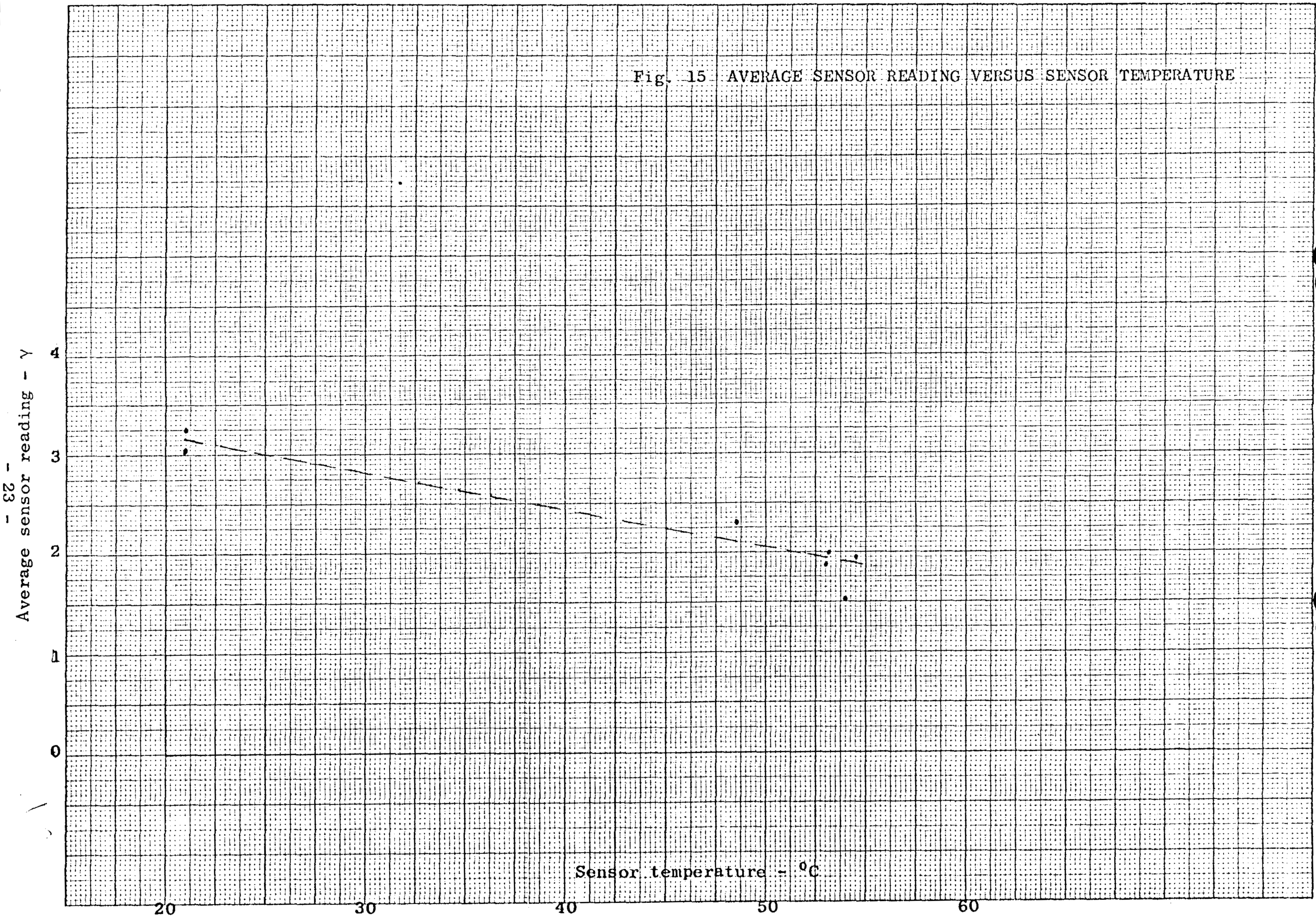

Fig. 15 AVERAGE SENSOR READING VERSUS SENSOR TEMPERATURE

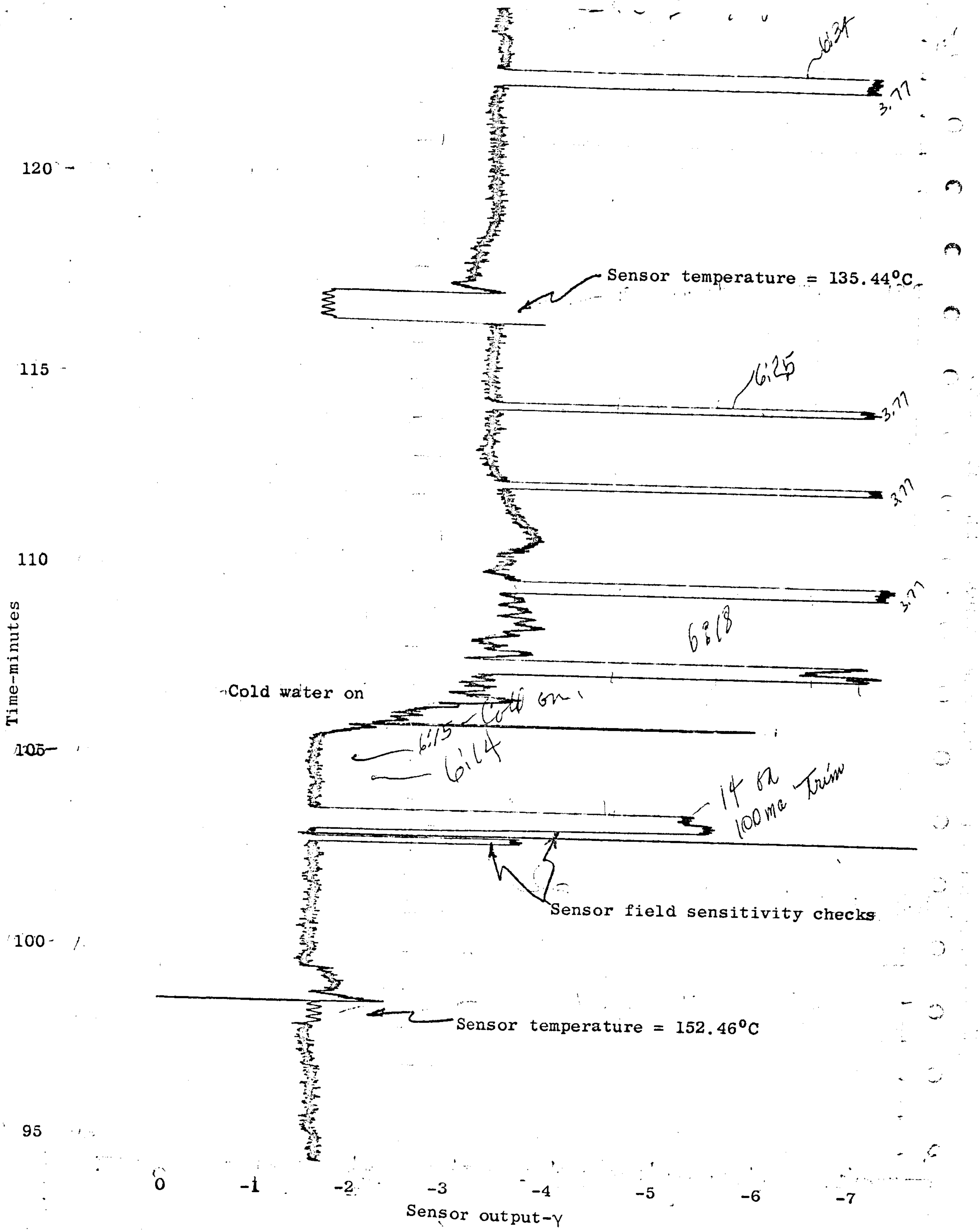

Fig. 16 TYPICAL RECORDER TRACE DURING TEMPERATURE CHANGE